

# Shear Behavior of Single Cast-in Anchors in Plastic Hinge Zones

Derek Petersen<sup>1)</sup>, Zhibin Lin<sup>2)</sup>, and Jian Zhao<sup>3)</sup>,\* 

(Received June 16, 2017, Accepted January 24, 2018)

**Abstract:** This paper presents two shear tests of 3/4-in. diameter cast-in anchors embedded in the plastic hinge zone of reinforced concrete columns. Design codes, such as ACI 318-14, require special reinforcement for concrete anchors in concrete that could be substantially damaged during an earthquake. The test anchors in this study were equipped with the anchor reinforcement recommended and verified in the literature. The column specimens were subjected to quasi-static cyclic loading before the test anchors were loaded in shear. Steel fracture was achieved in both test anchors despite cracks and concrete spalling occurred to the concrete within the plastic hinge zones. Meanwhile, the measured anchor capacities were smaller than the code-specified capacity, especially for the anchors subjected to cyclic shear. Concrete cover spalling was found critical to the observed capacity reduction, which caused combined bending and shear action in the anchor bolts. Measures should be developed to mitigate such adverse impact. In addition, further studies are needed for post-installed anchors before practical applications.

**Keywords:** cast-in anchors, anchor reinforcement, concrete anchor, studs, fastening to concrete, reinforced concrete, seismic design.

## 1. Introduction

Concrete anchors are needed to connect structural steel members and concrete. For example, reinforce concrete frames have been strengthened using steel braces (Badoux and Jirsa 1990), in which, the steel braces can be fixed to concrete beam/column ends using concrete anchors such as post-installed adhesive anchors or through bolts. The anchor bolts in such connections on the side faces of a concrete frame are subjected to cyclic shear during an earthquake, and the anchors have limited edge distance in the loading direction.

Typical failure modes for such anchors in shear are anchor steel fracture and concrete breakout failure (ACI 318, 2014). Anchor steel failure is caused by fracture of an anchor shaft in shear while concrete breakout failure is marked by a concrete cone broken away from the base concrete, in which the connection is located. Concrete breakout failure in shear occurs when anchors are located close to an edge. Concrete breakout is a brittle failure mode and thus not preferred for anchor connections in seismic zones (Petersen et al. 2013a). The well-established design procedures for concrete anchors, such as those stipulated in ACI 318-14, do not apply to the

anchors installed in plastic hinge zones. This is because the concrete in plastic hinge zones likely develops substantial damaged during an earthquake while the design procedures are based on experimental tests of anchors in concrete that is not significantly stressed/cracked.

Anchor reinforcement must be provided for the anchors installed in plastic hinge zones. V-shaped hairpins encasing the anchor shaft, as recommended in ACI 318-14 codes, may not be practical for embedded connections. With a goal to confine concrete around the shaft of an anchor in shear, Petersen and Zhao (2013) proposed new anchor shear reinforcement, consisting of closely spaced stirrups, corner bars, and crack-controlling bars. The proposed reinforcement has been proved effective for anchors placed in unstressed/un-cracked concrete. Meanwhile, beam/column ends, where anchor connections are placed, are likely to develop significant damages during an earthquake (Ibarra and Krawinkler 2005). The impact of potential severer damage in concrete on the effectiveness of the anchor reinforcement and on the behavior of anchors installed in plastic hinge zones has not been evaluated. In this paper, laboratory tests were presented to evaluate the recommended reinforcement for anchors installed in the plastic hinge zone of concrete columns.

## 2. Literature on Anchor Behavior in Damaged Concrete

The behavior of concrete anchors as a connection between steel members and concrete has been extensively studied as summarized in Cook and Klingner (1992), Grauvilardell et al. (2005), Eligehausen et al. (2006), and Pallarés and

<sup>1)</sup>Koppers Railroad Structures, 4546 Tompkins Dr., Madison, WI 53716, USA.

<sup>2)</sup>Department of Civil and Environmental Engineering, North Dakota State University, Fargo, ND 58105, USA.

<sup>3)</sup>Department of Civil and Environmental Engineering, University of Wisconsin, Milwaukee, WI 53211, USA.

\*Corresponding Author; E-mail: jzhao@uwm.edu

Copyright © The Author(s) 2018



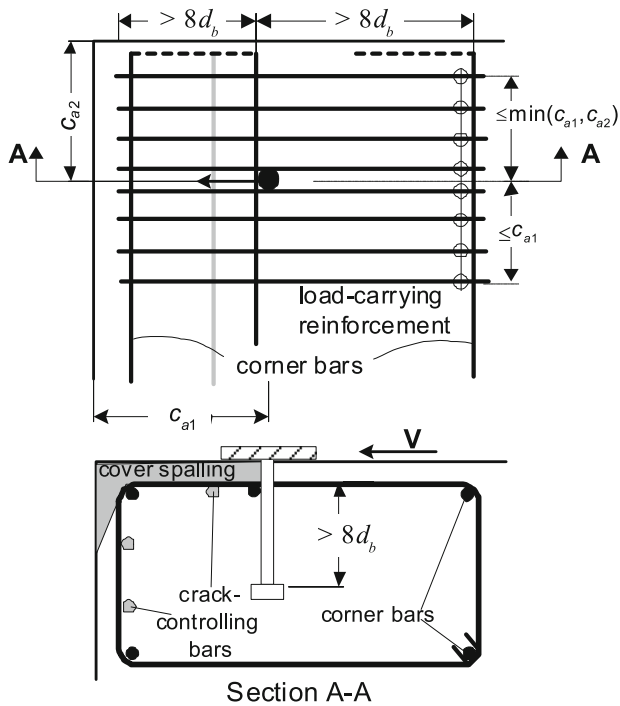


**Fig. 2** Proposed anchor shear reinforcement by Petersen and Zhao (2013).

sides of the anchor bolt, and a 90-degree bend as shown in dashed lines in Fig. 2 may be used.

In summary, the existing anchor studies in the literature do not reflect the damage concrete may experience in plastic hinge zones. In addition, anchor reinforcement has been proposed and verified using the tests in undamaged concrete. This paper presents two tests of cast-in anchors with the recommended anchor reinforcement in substantially damaged concrete.

### 3. Experimental Program

#### 3.1 Reinforced Concrete Column Specimen

A total of three reinforced concrete (RC) columns were used for the single anchors in plastic hinge zones. The RC columns had a section of  $305 \times 305$  mm [ $12 \times 12$  in.] and a height about 1.5 m [5 ft.] from the top face of the base block, as shown in Fig. 3. The column base block had a dimension of  $1219 \times 240$  mm [ $48 \times 20$  in.] and a height of 432 mm [17 in.]. Two tie-down holes were created using embedded PVC tubes. The tie down points were 0.91 m [3 ft.] from the center of the column, following the hole pattern in the strong floor of the University of Wisconsin-Milwaukee (UWM) Structures Laboratory. The horizontal loads were applied to the top of the column at 1.57 m [62 in.] from the base through a steel loading block.

Eight No. 5 bars (ASTM Grade 60) were provided as the longitudinal reinforcement for the columns. The concrete cover was 38 mm [1.5 in.], typical for RC members with exterior exposure. A section analysis with the actual material properties shown below indicated that the column had a nominal moment capacity about 105.8 kN-m [78 k-ft.]. This

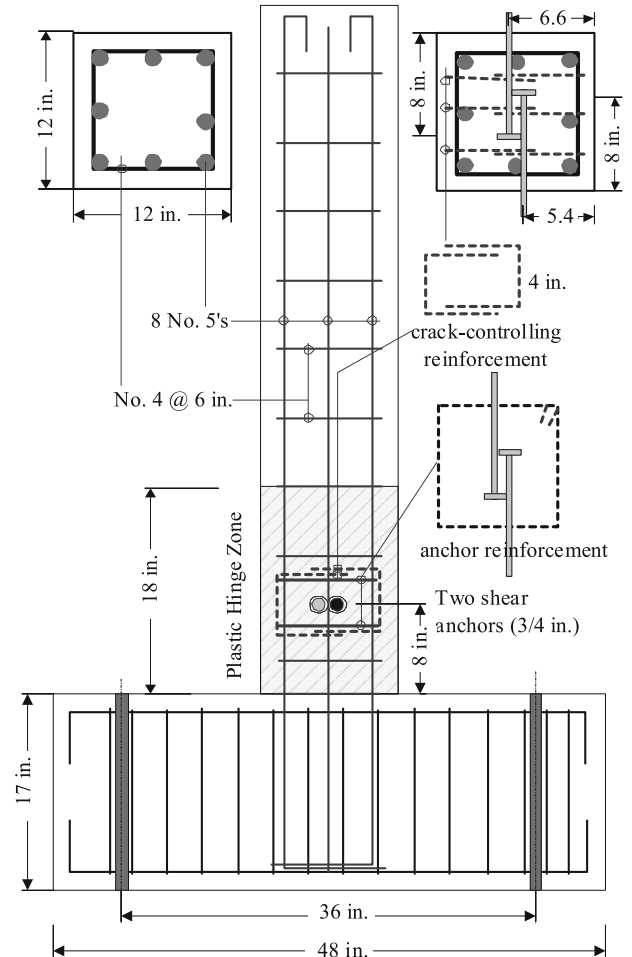


**Fig. 3** Dimension and reinforcement of shear specimens (1 in. = 25.4 mm).

corresponded to a lateral load capacity about 67.4 kN [15 kips] at the top of the column. A shear design calculation for this ultimate load led to No. 4 ties at a spacing of 152 mm [6 in.], as illustrated in Fig. 3.

#### 3.2 Test Anchors

Two anchors are placed in each column specimen and loaded in shear simultaneously. The test anchors were made from 19-mm [ $3/4$ -in.] diameter ASTM A193 Grade B7 threaded rods. The net shear area ( $A_{sa,v}$ ) for the threaded rods was  $2.2$  cm<sup>2</sup> [ $0.334$  in.<sup>2</sup>]. Each test anchor, if fully developed, has an ultimate shear capacity ( $V_u$ ) of 117 kN [26.4 kips]. Two single anchors, one installed on each side of the RC column, were loaded simultaneously to eliminate the torsion to the column. The test anchor had an embedded length ( $h_{ef}$ ) of 203 mm [8 in.], and located at the middle of the column side faces. With this configuration, one anchor would have a front edge distance of 138 mm [5.4 in.] while the other 167 mm [6.6 in.], as shown in Fig. 3. This difference in the front edge distance was expected to create small behavioral difference because of the anchor shear reinforcement placed near the test anchors.

The test anchor was installed 203 mm [8 in.] above the base block. The length of the plastic hinge zone was assumed as 0.46 m [18 in.] (that is 1.5 times the column

section height), as shown by shaded region in Fig. 3. The anchor position was selected assuming a crack spacing of 51 mm [2 in.] such that a major flexural crack would pass through the test anchor if the anchor reinforcement were not provided.

The design of the anchor shear reinforcement using strut-and-tie models is illustrated in Fig. 4. The required anchor reinforcement for the 19-mm [ $\frac{3}{4}$ -in.] anchors in shear was found to be 2.8 cm<sup>2</sup> [0.44 in.<sup>2</sup>], following the design method described in the previous section. Two No. 4 ties (with two stirrups legs perpendicular to the anchor as the load-carrying reinforcement) were provided: one located 51 mm [2 in.] above the test anchor and the other below the anchor, as shown in Fig. 3. The stirrups were not placed next to the test anchor as recommended by Petersen and Zhao (2013) due to a space limitation and the need for crack-controlling reinforcement. Two additional stirrups, located about 127 mm [5 in.] from the test anchors as shown in Fig. 3, may also be counted as anchor shear reinforcement; however, they were expected to be less effective compared with the two adjacent stirrups.

Crack-controlling reinforcement is important for the load carrying reinforcement to function. With the configuration shown in Fig. 4, the vertical splitting force from each anchor in shear, which might cause horizontal splitting cracks, was calculated as about 27 kN [6 kips]. The required crack-controlling reinforcement was 1.1 cm<sup>2</sup> [0.17 in.<sup>2</sup>] using  $0.6f_y$  where  $f_y$  is the yield strength of the bars. One No. 4 hairpin in the vertical plane, as shown in Fig. 3, was provided. Another No. 4 hairpin in the vertical plane was provided to resist the splitting force from the other anchor in shear. In addition, the column was expected to develop flexural cracks under lateral loading, especially in the plastic hinge zones. The cracks might propagate passing the test anchor. This cracking potential is in addition to that caused by the force applied to the test anchors. One additional hairpin was placed in the middle to restrain the flexural cracking near the anchors. The development length requirement for both the No. 4 ties and the U-shaped hairpins was assumed satisfied through the interaction between the closed ties and corner bars.

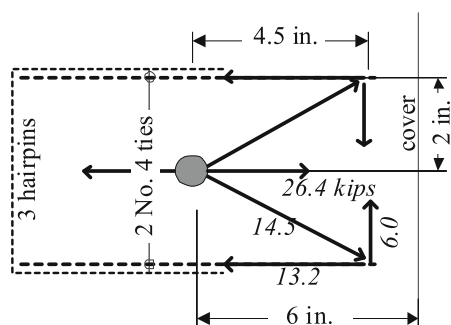


Fig. 4 Strut-and-tie models for the specimen design (1 in. = 25.4 mm; 1 kip = 4.45 kN).

### 3.3 Materials

Ready mixed concrete with Wisconsin Department of Transportation Type A-FA mixture was used. The specified concrete compressive strength was 27.6 MPa [4000 psi]. The hardened concrete had a compressive strength of 40 MPa [5800 psi] at 28 days, and the compressive strength went up to 47.6 MPa [6900 psi] at about 84 days, when the tests presented in this paper were conducted.

Eight No. 5 reinforcing steel bars with a nominal yield strength of 414 MPa [60 ksi] were used as longitudinal reinforcement. The measured stress-strain relationship, shown in dashed lines in Fig. 5a experienced a grip slip. A correction was performed based on the strain gage readings and the strains calculated from the measured elongation over a 203-mm [8-in.] gage length. The corrected stress-strain relationship, shown in solid lines in Fig. 5a, indicates a yield strength of 448 MPa [65 ksi] using the 0.2% offset method. The ultimate strength of the reinforcing bars was measured 696 MPa [101 ksi] at a strain about 0.15.

The stress-strain relationship of ASTM A193 Grade B7 rods was measured using the tensile test of a coupon made from a rod. Again, a grip slip was observed when the stress was above 620 MPa [90 ksi], as shown in Fig. 5b. No strain gage was used in this test; hence a correction was not performed. The measured yield strength was 724 MPa [105 ksi] corresponding to a 0.2 percent residual strain. The measured ultimate strength was 914 MPa [132 ksi] at a strain about 0.045.

### 3.4 Test Setup and Loading Protocol

The test setup is shown in Fig. 6. The column specimen was fixed to the strong floor of the laboratory using two high-strength threaded rods. An MTS Model 244.31, 245-kN [55-kip] actuator was used to apply a reversed cyclic displacement at the top of the column. The lateral load was applied to the column at 1.58 m [62 in.] above the base block. Another MTS Model 244.31 actuator was used to apply shear forces to the anchors through a loading adapter. The centerline of this actuator was located at the height of the test anchor. Strain gages and linear potentiometers were used to monitor the behavior of the test columns and the anchors. Specifically, the displacement at the column top was measured using a linear potentiometer mounted on a reference column. In addition, the anchor displacements were measured using two linear variable differential transformers (LVDT's) mounted on the loading plate with respect to the column surface as shown in Fig. 6. The instrumentation details can be found elsewhere (Petersen et al. 2013b).

The columns were subjected to reversed cyclic displacements. The displacement history included groups of three cycles with the peak displacements corresponding to  $\pm \Delta y$ ,  $\pm 2\Delta y$ ,  $\pm 3\Delta y$ ,  $\pm 4\Delta y$ ,  $\pm 6\Delta y$ , and  $\pm 8\Delta y$ . The yield displacement ( $\Delta y$ ) was determined using a fiber-based analysis of the column. The initial test results showed differences between the command displacements and the actual column displacements, and the peak displacements were slightly modified accordingly. The loading rate for

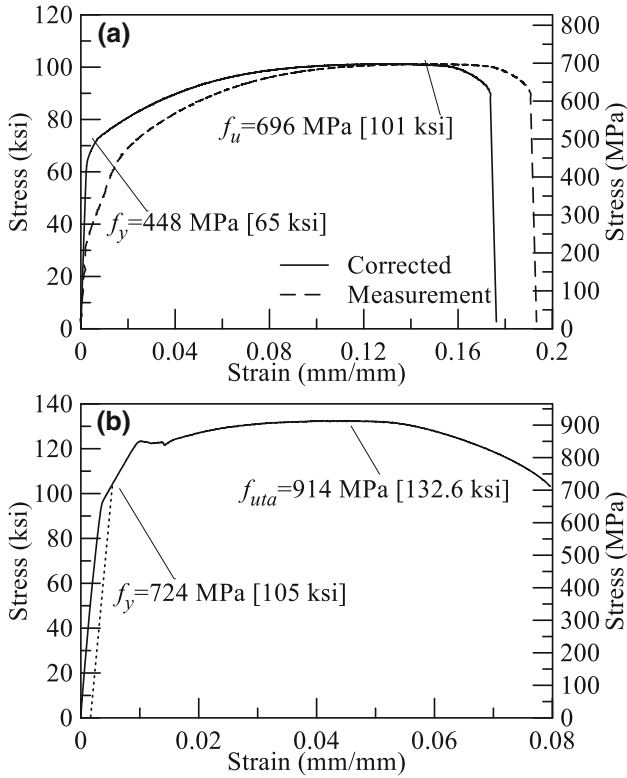


**Fig. 5** Materials used in test: **a** No. 5 Grade 60 rebar and **b** ASTM A193 Grade B7 rods.

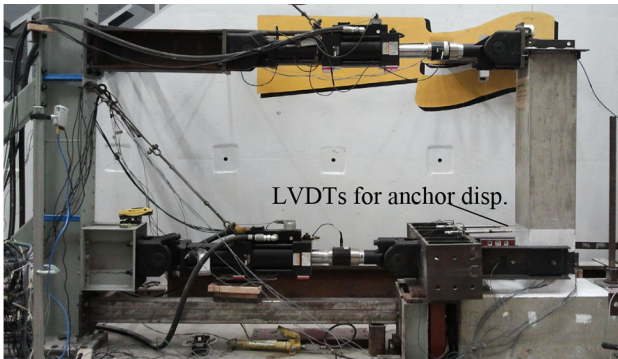


**Fig. 6** Test setup for shear tests of cast-in anchors in plastic hinge zone.

displacement cycles were kept at 6 mm/min [0.24 in./min] throughout the tests.

The anchors in Specimen S1 were loaded in monotonic shear till failure after the column was subjected to the pre-defined loading history described above. The anchors in Specimen S2 were loaded in reversed cyclic loading, and the peak displacements were determined based upon the results of the Specimen S1. The loading on the test anchors was in the same direction as the load on the column, as illustrated later in Fig. 9.

The test specimen could fail in several possible failure modes under the complex combination of column loading and anchor loading. Design checks for the column were conducted for a variety of failure modes to ensure that column specimen would not fail before the testing anchor reached at its full design capacity. These failure modes included flexural and shear failure of the column under the

load from the test anchors. In addition, shear friction along flexural cracks was found unlikely to control the failure of the test. Details about the design checks can be found elsewhere (Zhao 2014) while similar design calculations are recommended for design practices.

### 3.5 Shear Capacity Prediction

The full shear capacity of the anchors, according to ACI 318-14, was calculated from

$$V_{se} = 0.6f_{uta}A_{se,V} \quad (1)$$

where  $f_{uta}$  is the ultimate tensile strength of the anchor steel and  $A_{se,V}$  is the net shear area of the anchor shaft. However, this calculation overestimated the actual shear capacity because the cover concrete was lost during the test, and the anchors had an exposed length. In this case, several equations have been proposed to calculate the shear capacity of anchor bolts with an exposed length  $l$ . For example, Eligehausen et al. (2006) proposed the following equation,

$$V_{se} = 2 \frac{1.7Sf_{ya}}{l} \quad (2)$$

while a different model was proposed by Lin et al. (2011),

$$V_{se} = f_{ya}A_{se,v} \sin(\beta) + \frac{f_{ya} \cos(\beta)}{\frac{1}{0.9A_{se,v}} + \frac{l}{3.4S}} \quad (3)$$

where  $f_{ya}$  is the yield strength of anchor steel,  $S$  is the section modulus of the test anchor, and the rotation angle of the exposed anchor ( $\beta$ ) is estimated as  $\theta + l_p \tan^{-1} \frac{\epsilon_{max}}{d_a}$ , in which the maximum tensile strain ( $\epsilon_{max}$ ) was obtained from the anchor material;  $\theta$  is the initial end rotation allowed by the oversized holes and/or concrete deformation,  $l_p$  is the length of plastic hinge developed in anchor shaft at the ultimate load, and may be taken as  $d_a$  (nominal diameter of the anchor).

To avoid friction between load plate and concrete surface during the test, a 3-mm [1/8-in.] gap was controlled between the loading plate and the concrete surface. Therefore, the exposed length for the anchor in this study could be between 3 mm [1/8 in.] and 41 mm [1.6 in.], which was the concrete cover depth. The calculated anchor shear capacity using Eq. 3 was thus between 64 kN [14.4 kips] and 122 kN [27.5 kips] depending upon the damage to the concrete cover around the test anchors. Equation (2) was proposed for anchors with a minimum exposed length of  $\frac{d_a}{2}$ , where  $d_a$  is the anchor diameter. Hence the predicted shear capacity was 41 kN [9.2 kips] for the test anchors with an exposed length of 41 mm [1.6 in.].

## 4. Discussion of Test Results

### 4.1 Column Surface Cracks

The column in Specimen S1 had a typical hysteretic behavior found in flexural members. An examination of the strains in the middle longitudinal bar indicated that the first

yield occurred during the loading cycle at about 13 mm [0.5 in.]. The largest column displacement was about 102 mm [4 in.], corresponding to  $8\Delta_y$ , at a peak load about 67 kN [15 kips]. The load–displacement behavior of Column S2 was affected by the simultaneous loading to the anchors.

The crack map of Column S1 is shown in Fig. 7 after all column loading cycles completed. While the crack maps after each loading group can be found elsewhere (Lin et al. 2013), a brief description of crack development is provided as follows: flexural cracks first developed at the base and within the plastic hinge zone. Smaller cracks were then observed at higher location with the increase of the loading level. The cracks in the plastic hinge zone widened and propagated upon further loading. Note that the column base crack is a result of yield penetration of steel reinforcing bars in the foundation. The crack width at the base of the columns was 0.3–0.5 mm [0.01–0.02 in.] at first yielding, which is close to the bar yield slip predicted by Zhao and Sritharan (2007). More cracks developed throughout the column during the following loading cycles. The crack widths in Fig. 7 were recorded after the  $\pm 8\Delta_y$  loading cycles. The largest crack at the column base was 8.0 mm [0.31 in.], which is slightly less than the ultimate bar slip recommended by Zhao and Sritharan (2007). Another crack at 102 mm [4 in.] above the base had a width of about 7 mm [0.27 in.].

The strains in the middle longitudinal bar are shown in Fig. 7a at the first peak of the  $\pm 8\Delta_y$  loading cycles, when the crack widths in Fig. 7b were recorded. The crack widths in millimeters, measured on the column faces, were listed in

Fig. 7b on the corresponding side of the column. The plastic high zone, shown by the shaded region, was 610 mm [24 in.] high, which is roughly twice the column section height. The largest crack width was 0.4 mm [0.06 in.] outside this region. Note that the design equations for concrete anchors in ACI 318-14 were established based on tests of both cast-in anchors and post-installed anchors in cracked and un-cracked concrete; meanwhile, the crack width in the tests have been limited to 0.5 mm [0.02 in.] to represent the condition of concrete at serviceability limit state. (Hoehler and Eligehausen 2008; Mahrenholtz et al. 2017). The observations in Fig. 7 support the current design regulations that the equations in ACI 318-14 should be used outside the plastic hinge zones, defined as twice the member depth from a column or beam face.

## 4.2 Anchor Behavior in Shear

### 4.2.1 Monotonic behavior in Specimen S1

The behavior of the two single anchors subjected to monotonic shear is shown in Fig. 8. The east anchor had a slightly larger shear displacement as shown in Fig. 8a partly because of a smaller edge distance. The X-axis thus shows the average shear displacement measured relative to the concrete front face in the load–displacement curve in Fig. 8b. The Y-axis shows the total shear resistance from the two single anchors. The anchors behaved elastically till about 33.4 kN [7.5 kips], beyond which the slope reduced significantly, indicating the crush of concrete in front of the anchor shafts. Cracks on the east side face first showed up at a load of 89 kN [20 kips] followed by spalling of concrete cover as shown later in Fig. 10. Meanwhile, the cover cracks on the west side were arrested by an existing flexural crack, and the cracked concrete pieces were not significantly crushed. This indicated that the west side anchor had a relatively better lateral support than the east anchor, thus a higher shear capacity.

The shear force increased with a relatively high slope beyond 111.2 kN [25 kips] corresponding to a displacement about 19 mm [0.75 in.]. Similar observation has been made in a previous study (Petersen and Zhao 2013): the anchor shafts bent when the concrete cover spalled, and carried the shear load partially in tension. Therefore, the final anchor shear capacity had contributions from anchor shaft in shear, bending, and tension as indicated by Eq. 3. The east anchor fractured while the west anchor was also significantly bent, when the combined load was 175 kN [39.4 kips]. On average, each anchor had a shear capacity of 87.5 kN [19.7 kips], which is within the predicted range shown above. An after-test examination indicated that the unsupported length of the anchor shafts was 38 mm [1.5 in.] at the east side and 25 mm [1.0 in.] at the west side, which were measured after the crushed concrete around the anchor shafts was removed.

The average shear capacity of 87.5 kN [19.7 kips] is much higher than the code-specified breakout capacity (38 kN [8.6 kips]), which would have controlled the anchor behavior if the anchor reinforcement were not provided. Anchor steel fracture was achieved because of the well-

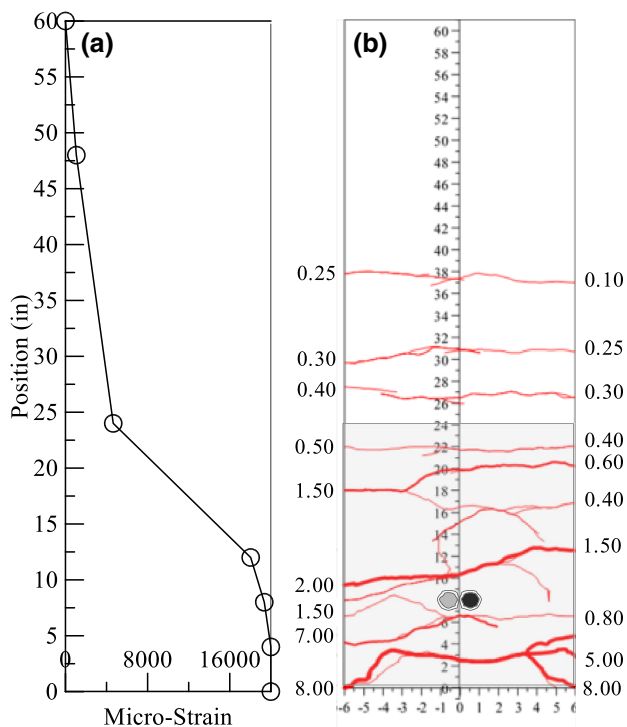


**Fig. 7** Strain in a longitudinal bar and crack map of Specimen S1 column at  $8\Delta_y$  (Crack width in mm; 1 in. = 25.4 mm). **a** Strains in longitudinal bars and **b** crack map (crack widths shown on the side of column).

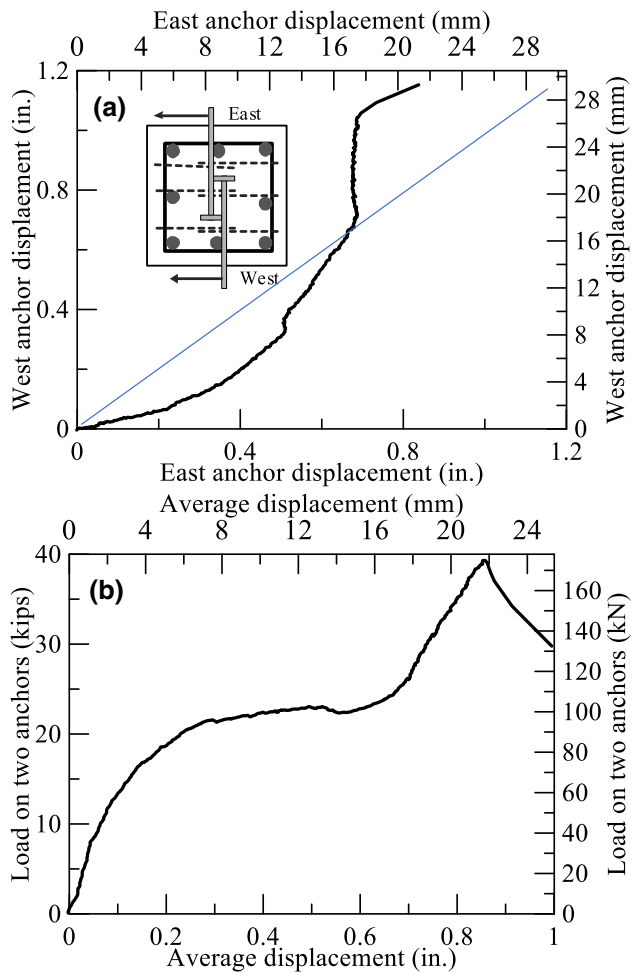


**Fig. 8** Behavior of single anchor in plastic hinge zone under monotonic shear loading. **a** Comparison of measurements from two LVDT's and **b** load vs average displacement curve.

confined core concrete in the plastic hinge zone of the column specimen. The core concrete was protected with the provided anchor reinforcement though the column outside the concrete core had significant damage.

#### 4.2.2 Cyclic behavior in Specimen S2

The anchors in Specimen S1 failed in shaft fracture after the concrete cover spalled. The spalling was partially attributed to the damage to the concrete in the plastic hinge zone after the column was subjected to large inelastic deformation. Anchor connections are loaded along with concrete structures in reality; therefore the test of Specimen S2 was slightly modified: both the column and the anchors were subjected to loading simultaneously. The loading protocol for the column stayed the same as Specimen S1, while a displacement loading protocol was created based on the observed behavior in Specimen S1 (Fig. 8b). Note that the actuator that applied shear loading to the test anchors was not controlled based on the measured anchor displacement due to equipment limitations; hence the actual anchor displacements were difference from the actuator displacement.

The cyclic behavior of Specimen S2 is plotted in Fig. 9a. Again, the displacement in the plot is the average

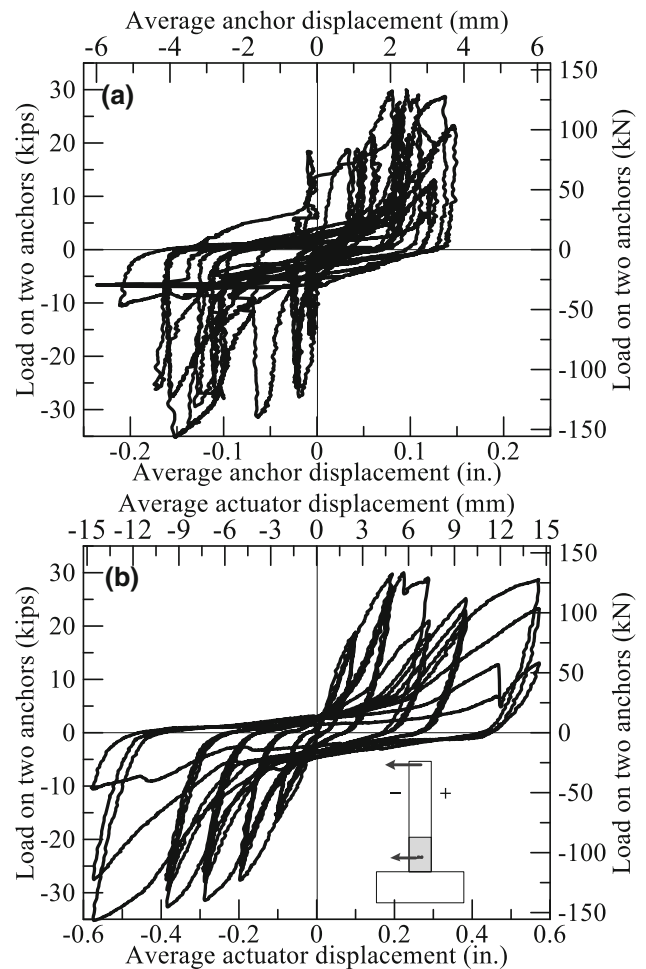


**Fig. 9** Behavior of single anchor in plastic hinge zone under cyclic shear loading. **a** load vs anchor displacement measured by LVDT's and **b** load vs anchor displacement measured by actuator.

displacement measured from two linear variable differential transformers (LVDT's), and the load is the combined shear resistance from two test anchors. The overall anchor behavior displayed pinching effects because the concrete, crushed in front of the anchor shafts during the initial loading, did not recover its lateral support to the shafts upon unloading and reloading. In addition, the anchor behavior was slightly under the shear loading in two directions: the measured anchor shear capacity was 131 kN [29.4 kips] when the actuators were in tension while the capacity was 157 kN [35.2 kips] when the actuators were in compression. The lateral deformation of the column at 8 in. above base and the related rotation may have been partly responsible to the slight difference.

Unlike Specimen S1, the concrete cover spalling did not occur at early stage of loading; hence the load–displacement curve of Specimen S2 does not show an apparent “yield point” at about 89 kN [20 kips], beyond which the loading capacity remained unchanged with an increase in the anchor displacement. The stiffness of Specimen S2 reduced significantly at a higher load about 129 kN [29 kips]. Beyond the point, the anchor behavior was stable for several groups of displacement cycles from the load vs actuator displacement



addition to distributing loads from the anchor to the rest of the structure/structural element.

The anchors developed steel fracture instead of concrete breakout failure despite large cracks and concrete spalling occurred to the surrounding concrete. The successful tests indicated that well confined core concrete, even within plastic hinge zones, can support anchor connections in shear. Meanwhile, concrete cover spalled during the tests, adversely impacted the anchor shear behavior. Further research is needed to protect cover concrete for connection with concrete anchors to achieve desired behavior. In addition, further studies are needed for post-installed anchors, which are widely used in structural retrofit.

## Acknowledgments

The study reported in this paper is from a project funded by the National Science Foundation (NSF) under Grant No. 0724097. The authors gratefully acknowledge the support of Dr. Joy Pauschke, who served as the program director for this grant. Any opinions, findings, and recommendations or conclusions expressed in this paper are those of the authors, and do not necessarily reflect the views of NSF.

## Open Access

This article is distributed under the terms of the Creative Commons Attribution 4.0 International License (<http://creativecommons.org/licenses/by/4.0/>), which permits unrestricted use, distribution, and reproduction in any medium, provided you give appropriate credit to the original author(s) and the source, provide a link to the Creative Commons license, and indicate if changes were made.

## References

- American Concrete Institute (ACI) Committee 318. (2011). *Building code requirements for structural concrete (ACI 318-14)*. MI: Farmington Hills.
- Badoux, M., & Jirsa, J. (1990). Steel bracing of RC frames for seismic retrofitting. *ASCE Journal of Structural Engineering*, 116(1), 55–74.
- Cook, R. A., & Klingner, R. E. (1992). Ductile multiple-anchor steel to-concrete connections. *Journal of Structural Engineering*, 118(6), 1645–1665.
- Eligehausen, R., Mällée, R., & Silva, J. (2006). *Anchorage in Concrete Construction*. Berlin, Germany: Wilhelm Ernst & Sohn.
- Grauvilardell, J., Lee, D., Hajjar, J., Dexter, R. (2005). Synthesis of design, testing and analysis research on steel column base plate connections in high-seismic zones. *Structural Engineering Report No. ST-04-02*. Minneapolis: University of Minnesota.
- Hoehler, M. S., & Eligehausen, R. (2008). Behavior and testing of anchors in simulated seismic cracks. *ACI Structural Journal*, 105(3), 348–357.
- Ibarra L. F., Krawinkler, H. (2005). Global collapse of frame structures under seismic excitations, Report No. TB 152, The John A. Blume Earthquake Engineering Center, Stanford University, Stanford.
- Klingner, R., Mendonca, J., & Malik, J. (1982). Effect of reinforcing details on the shear resistance of anchor bolts under reversed cyclic loading. *ACI Journal*, 79(1), 471–479.
- Lee, N., Park, K., & Suh, Y. (2010). Shear behavior of headed anchors with large diameters and deep embedment. *ACI Structural Journal*, 108(1), 34–41.
- Lin, Z., Luke, B., Shahrooz, B., and Zhao, J. (2013). Headed anchors in plastic hinge zone of reinforced concrete members. Final report (Volume III) for project—behavior and design of cast-in-place anchors under simulated seismic loading. Milwaukee: University of Wisconsin.
- Lin, Z., Petersen, D., Zhao, J., & Tian, Y. (2011). Simulation and design of exposed anchor bolts in shear. *International Journal of Theoretical and Applied Multiscale Mechanics*, 2, 111–119.
- Mahrenholtz, C., Eligehausen, R., Hutchinson, T., & Hoehler, M. (2017). Behavior of post-installed anchors tested by stepwise increasing cyclic crack protocols. *ACI Structural Journal*, 114(3), 621–630.
- Nakashima, S. (1998). Mechanical characteristics of exposed portions of anchor bolts subjected to shearing forces summaries of technical papers of annual report. *Architectural Institute of Japan*, 38, 349–352.
- Oehlers, D., & Park, S. (1992). Shear connectors in composite beams with longitudinally cracked slabs. *Journal of the Structural Engineering*, 118(8), 2004–2022.
- Pallarés, L., & Hajjar, J. (2010). Headed steel stud anchors in composite structures, part I: shear. *Journal of Constructional Steel Research*, 66(2), 198–212.
- Petersen, D., Lin, Z., Zhao, J. (2013a). Reinforcement for headed anchors. Final report (Volume I) for project—behavior and design of cast-in-place anchors under simulated seismic loading. Milwaukee: University of Wisconsin.
- Petersen, D., Lin, Z., Zhao, J. (2013b). Reinforcement for headed anchors. Final report (Volume II) for project—behavior and design of cast-in-place anchors under simulated seismic loading. Milwaukee: University of Wisconsin.
- Petersen, D., & Zhao, J. (2013). Design of anchor reinforcement for seismic shear loads. *ACI Structural Journal*, 110(1), 53–62.
- Saari, W., Hajjar, J., Schultz, A., & Shield, C. (2004). Behavior of shear studs in steel frames with reinforced concrete infill walls. *Journal of Constructional Steel Research*, 60(10), 1453–1480.
- Zhang, Y., Klingner, R. E., & Graves, H. L., III. (2001). Seismic response of multiple-anchor connections to concrete. *ACI Structural Journal*, 98(6), 811–822.
- Zhao, J. (2014). Seismic behavior of single anchors in plastic hinge zones of RC columns. Tenth U.S. National

Conference on Earthquake Engineering Frontiers of Earthquake Engineering July 21–25, 2014 Anchorage, Alaska.

Zhao, J., & Sritharan, S. (2007). Modeling of strain penetration effects in fiber-based analysis of reinforced concrete structures. *ACI Structural Journal*, 104(2), 1–7.